Previously uncharacterized roles of platelet-activating factor acetylhydrolase 1b complex in mouse spermatogenesis

Wei Yan*†, Amir H. Assadi†‡, Anthony Wynshaw-Boris§, Gregor Eichele¶‖, Martin M. Matzuk*,††, and Gary D. Clark‡,‡‡§§¶¶**

Departments of *Pathology, ‡Pediatrics, ¶Biochemistry, **Molecular and Cell Biology, ††Molecular and Human Genetics, and ‡‡Neurology and Neuroscience and §§Cain Foundation Laboratories, Baylor College of Medicine, Houston, TX 77030; and §Departments of Pediatrics and Medicine, University of California at San Diego, La Jolla, CA 92093-0627

Edited by David L. Garbers, University of Texas Southwestern Medical Center, Dallas, TX, and approved April 18, 2003 (received for review October 10, 2002)

Platelet-activating factor (PAF) has been shown to affect sperm motility and acrosomal function, thereby altering fertility. PAF acetylhydrolase 1b (PAFAH1B) hydrolyzes PAF and is composed of three subunits [the lissencephaly (LIS1) protein and α1 and α2 subunits] and structurally resembles a GTP-hydrolyzing protein. Besides the brain, transcripts for Lis1, α1, and α2 are localized to meiotic and early haploid germ cells. Here, we report disruptions of the α2 (*Pafah1b2*) and α1 (*Pafah1b3*) genes in mice. Male mice homozygous null for α2 ($\alpha2^{-/-}$) are infertile, and spermatogenesis is disrupted at mid- or late pachytene stages of meiosis or early spermiogenesis. Whereas mice homozygous mutant for α1 ($\alpha1^{-/-}$) have normal fertility and normal spermatogenesis, those with disruptions of both α1 and α2 ($\alpha1^{-/-}\alpha2^{-/-}$) manifest an earlier disturbance of spermatogenesis with an onset at preleptotene or leptotene stages of meiosis. Testicular Lis1 protein levels are up-regulated in the $\alpha2^{-/-}$ and $\alpha1^{-/-}\alpha2^{-/-}$ mice. Lowering Lis1 levels by inactivating one allele of Lis1 in α2 null or $\alpha1/\alpha$ 2 null genetic backgrounds (i.e., $\alpha2^{-/-}$Lis1$^{+/-}$ or $\alpha1^{-/-}\alpha2^{-/-}$Lis1$^{+/-}$ mice) restored spermatogenesis and male fertility. Our data provide evidence for unique roles of the PAFAH1B complex and, particularly, the lissencephaly protein Lis1 in spermatogenesis.

testis | apoptosis | lissencephaly

Mammalian male fertility depends on the generation of motile spermatozoa through the process of spermatogenesis, which involves mitosis, meiosis, and spermiogenesis (1). Both extragonadal hormones and intragonadal factors participate in the regulation of spermatogenesis. The signals mediated by these factors converge on an intracellular signaling machinery, which determines the fates of male germ cells. Knockout studies over the past 10 years have defined key roles of many extracellular and intracellular signaling proteins in reproductive physiology (2).

Platelet-activating factor (PAF or 1-*O*-akyl-2-*O*-acetyl-*sn*-glycero-3-phosphorylcholine) is one of the most potent lipid messengers involved in a variety of physiological events. PAF has been implicated in proper sperm motility (3, 4) and acrosomal function (5). The major regulatory enzymes for PAF biosynthesis via the *de novo* pathway, including acetyltransferase and cholinephosphotransferase, are present in spermatozoa (6). A role for PAF in the pathogenesis of testicular ischemia also has been suggested (7); however, PAF has not been implicated in spermatogenesis.

The acetyl group at the sn-2 position of the glycol backbone of PAF is essential for its biological activity, and its deacetylation induces loss of activity. The deacetylation reaction is catalyzed by PAF-acetylhydrolases (PAFAH). There are at least three types of PAFAH in mammals, namely, the intracellular types I and II and a plasma type (8). Type I PAFAH is a G protein-like complex consisting of two catalytic subunits (α1 and α2) and a regulatory β-subunit (8). The β-subunit is a product of the *LIS1* gene, mutations of which cause classic lissencephaly (9). Recent studies indicate that LIS1 is important in cellular functions such as induction of nuclear movement and control of microtubule organization (8). Although evidence is accumulating that the catalytic subunits are involved in microtubule function, it is still unknown whether PAF functions in this process or is an endogenous substrate of this enzyme. Mice homozygous null for *Lis1* die early in embryogenesis soon after implantation, whereas mice with one active allele display multiple neuronal migration defects (10).

In this study, we report that disruptions of the α2 and α1 genes and genetic interactions with Lis1 impair spermatogenesis in mice. We demonstrate further that inactivation of one allele of Lis1 in $\alpha2^{-/-}$ or $\alpha1^{-/-}\alpha\ 2^{-/-}$ mutant mice restores spermatogenesis and male fertility.

Materials and Methods

Generation and Genotype Analysis of the Mutant Mice. Disruption of the *Pafah1b3* gene (herein called α1) was made by replacement of the exonic sequence encoding the active enzyme site with a human *HPRT* minigene under control of a *Pgk* promoter (11, 12).

Disruption of *Pafah1b2* (herein called α2) was achieved by using a modified gene-trapping strategy in a 129S6/SvEv background (Lexicon Genetics, The Woodlands, TX). This targeting results in the duplication of genomic sequence, and, between the duplication, proprietary sequences were inserted that include a *Pgk1* promoter linked to puromycin *N*-acetyltransferase, a polyadenylation sequence, a splice acceptor fused to an internal ribosome entry site, and a galactosidase/neomycin phosphotransferase fusion gene (13). Genotyping for α1 and α2 was performed by Southern blot analysis (Fig. 1 *b* and *c*).

Genotyping of the *Pafah1b1* locus (herein called Lis1) was performed by using PCR as described (10).

Histology. Testes and epididymides were dissected, fixed in Bouin's fixative, embedded in paraffin, sectioned (5 μm), and stained with hematoxylin/eosin as described (12).

RNA Analysis. PCR-generated fragments of Lis1 (nucleotides 251–874, GenBank accession no. XM_109240), α1 (nucleotides

This paper was submitted directly (Track II) to the PNAS office.

Abbreviations: LIS1, lissencephaly protein 1; PAF, platelet-activating factor; PAFAH1B, PAF acetylhydrolase 1b; TUNEL, terminal deoxynucleotidyltransferase-mediated dUTP-biotin nick end labeling; P*n*, postnatal day *n*.

†W.Y. and A.H.A. contributed equally to this work.

‖Present address: Max Planck Institute, 30625 Hannover, Germany.

¶¶To whom correspondence should be addressed at: Department of Pediatrics, Neurology and Division of Neuroscience, Cain Foundation Research Laboratories, Baylor College of Medicine, 1102 Bates Street, Houston, TX 77030. E-mail: gclark@bcm.tmc.edu.

GENETICS

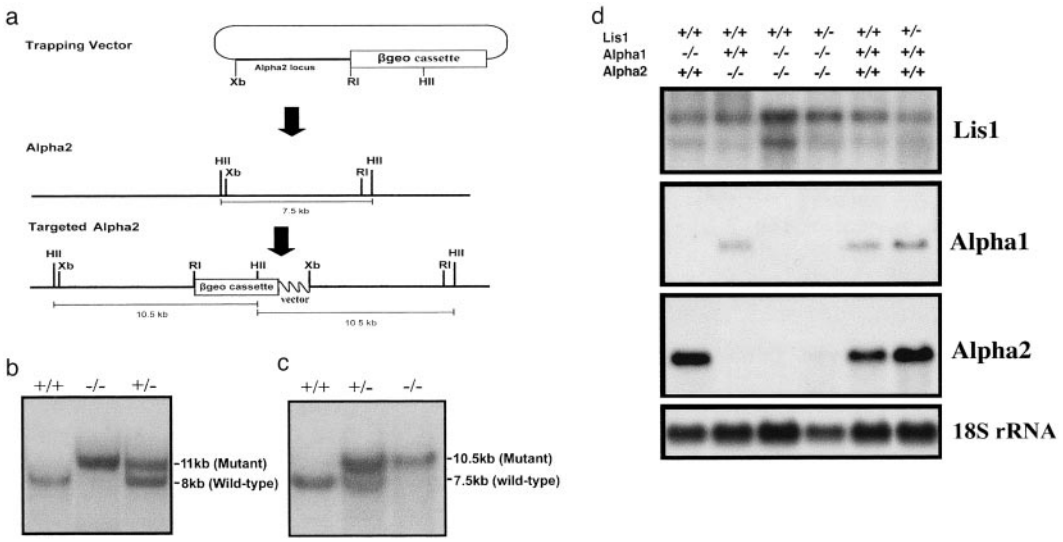

Fig. 1. α1 and α2 null mice. (*a*) Genomic organization of the wild-type and mutant α2 alleles and the structure of the targeting vector. (*b*) Southern blot analysis of α1 by using *Bam*HI-digested genomic DNA and 3′ probe (11). (*c*) Southern blot analysis of α2 by using a *Hin*dII-digested genomic DNA and a cDNA probe for encoding sequences of exons 3–5. The mutant allele is recognized as a 10.5-kb duplicate band and the wild-type allele is recognized as a 7.5-kb band. (*d*) Northern blot analysis of Lis1, α1, and α2 mRNAs and 18S rRNA in testes of wild-type and mutant mice.

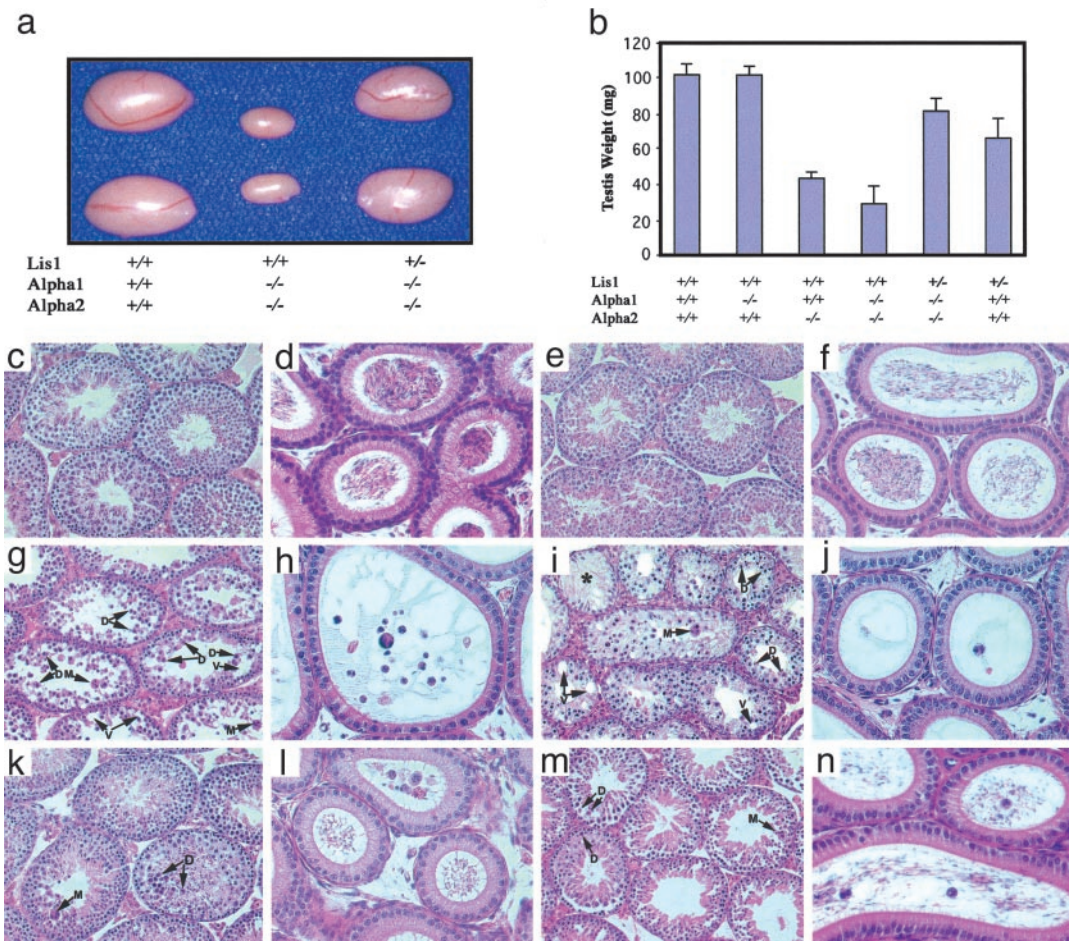

Fig. 2. Gross and histological analyses of spermatogenic abnormalities. (*a*) Reduced testis size in double-mutant mice ($\alpha1^{-/-}\alpha2^{-/-}$) and restored testis size in triple-mutant mice ($\alpha1^{-/-}\alpha2^{-/-}$Lis1$^{+/-}$). (*b*) Testis weights of 8-week-old wild-type and mutant mice (means ± SEM, $n = 10$). (*c*–*n*) Testicular (×200 in *c*, *e*, *g*, *i*, *k*, and *m*) and epididymal (×200 in *d*, *f*, *h*, *j*, *l*, and *n*) histology of adult (8-week-old) wild-type (*c* and *d*), $\alpha1^{-/-}$ (*e* and *f*), $\alpha2^{-/-}$ (*g* and *h*), $\alpha1^{-/-}\alpha2^{-/-}$ (*i* and *j*), $\alpha1^{-/-}\alpha2^{-/-}$Lis1$^{+/-}$ (*k* and *l*), and Lis1$^{+/-}$ (*m* and *n*) mice. Note that the degenerating germ cells (D), multinucleated giant cells (M), and numerous vacuoles (V) are present in tubules of the testes of $\alpha2^{-/-}$ (*g*), $\alpha1^{-/-}\alpha2^{-/-}$ (*i*), $\alpha1^{-/-}\alpha2^{-/-}$Lis1$^{+/-}$ (*k*), and Lis1$^{+/-}$ (*m*) mice. Some tubules are devoid of germ cells (*), leaving only Sertoli cells in the seminiferous epithelium in $\alpha1^{-/-}\alpha2^{-/-}$ mice (*i*).

98–653, GenBank accession no. NM_008776), and α2 (nucleotides 146–799, GenBank accession no. XM_134801) were subcloned into pGEM-T vector (Promega) followed by sequencing. Riboprobes were generated by using RiboProbe *in vitro* transcription systems (Promega) according to manufacturer instructions. Bouin's-fixed testis sections (5 μm) were used for *in situ* hybridization and autoradiography as described (14). Northern blot analysis was performed as described (15).

Western Blot Analysis. Testis protein was isolated by using T-PER Tissue Protein Extraction Reagent (Pierce) according to manufacturer instructions. Aliquots of 100 μg of protein were fractionated on 12.5% SDS-polyacrylamide gels and transferred to a nitrocellulose membrane (Schleicher & Schuell). Immunodetection was performed as described (16). The rabbit anti-LIS1 polyclonal antibody (N-19; Santa Cruz Biotechnology) was used at a dilution of 1:500. The membrane subsequently was stripped and blotted with an anti-actin mAb (ICN) for monitoring the loading. Quantitative analysis of Western blot results was performed as described (17).

Terminal Deoxynucleotidyltransferase-Mediated dUTP-Biotin Nick End Labeling (TUNEL) Analysis. Bouin's-fixed sections were used for TUNEL of apoptotic cells by the ApoTag Plus peroxidase kit (Intergen, Purchase, NY) according to manufacturer instructions.

Results and Discussion

In contrast to the embryonic lethality observed in Lis1$^{-/-}$ mice (10), α1$^{-/-}$ and α2$^{-/-}$ mice appeared developmentally normal, and expected Mendelian ratios of 1:2:1 were noted for heterozygote intercrosses of both, indicating that neither α1 nor α2 is required for embryonic and early postnatal development. Northern blot analysis of testes demonstrated that no mRNAs for α1 and α2 were produced in the α1$^{-/-}$ and α2$^{-/-}$ mice, respectively (Fig. 1*d*), demonstrating that α1 and α2 alleles were null for this tissue.

Testicular Phenotypes of Single-, Double-, and Triple-Mutant Mice. All morphological analyses were based on evaluation of at least five mice for each genotype group at the age of 8 weeks. α1$^{-/-}$ male and female mice bred normally. Testis weights of the adult α1$^{-/-}$ mice (103.7 $\pm$ 4.8 mg, n = 10) were similar to that of adult wild-type mice (103.8 $\pm$ 6.2 mg, n = 10) (Fig. 2*b*). Similar to the wild-type testis (Fig. 2 *c* and *d*), the α1$^{-/-}$ testis displayed robust spermatogenesis (Fig. 2*e*), and the epididymis was full of spermatozoa (Fig. 2*f*). α2$^{-/-}$ females bred normally, whereas α2$^{-/-}$ males were infertile when examined over a period of 6 months. The testis weights of α2$^{-/-}$ mice (44.9 $\pm$ 3.7 mg, n = 10) were 43% of wild-type testes at 8 weeks of age (Fig. 2*b*). In contrast to α1$^{-/-}$ mice, the seminiferous tubules of α2$^{-/-}$ testes were severely depleted of germ cells (Fig. 2*g*). Elongating and elongated spermatids were absent in the tubules, whereas spermatogonia and early spermatocytes appeared normal. Numerous degenerating and detaching pachytene spermatocytes and some multinucleated giant cells, which were syncytia of degenerating spermatids (18–21), were present throughout the seminiferous epithelium (Fig. 2*g*). Numerous vacuoles, representing vacuolated Sertoli cells resulting from severe germ cell depletion, are present in the epithelium. Some degenerating spermatocytes and spermatids detached from the seminiferous epithelium, sloughed into the tubule lumen, and were visible in the epididymis (Fig. 2*h*).

To determine whether there was redundancy of α1 and α2, we generated mice homozygous null for α1 and α2 (herein called double-mutant mice). Double-mutant females were grossly normal and fertile, whereas double-mutant males were infertile. Testicular weights of double-mutant males (30.6 $\pm$ 9.2 g, n = 10) were decreased further (<30% of wild-type testes) (Fig. 2 *a* and *b*), and germ cell depletion (Fig. 2 *i* and *j*) was more severe than in α2$^{-/-}$ testes. In the double-mutant testes, tubular structures were less obvious and the lumen was small. Most spermatids and pachytene spermatocytes were already depleted, leaving fewer germ cells in the seminiferous epithelium, and degenerated germ cells were visible in the epididymis (Fig. 2*j*). Some multinucleated giant cells, numerous degenerating preleptotene, leptotene, zygotene, and early pachytene spermatocytes, as well as multiple vacuoles were observed in the tubules. Some tubules were even completely devoid of germ cells, leaving only Sertoli cells (Fig. 2*i*), reminiscent of human "Sertoli cell-only" syndrome (2).

To define further the interactions of α1 and α2 with Lis1, we

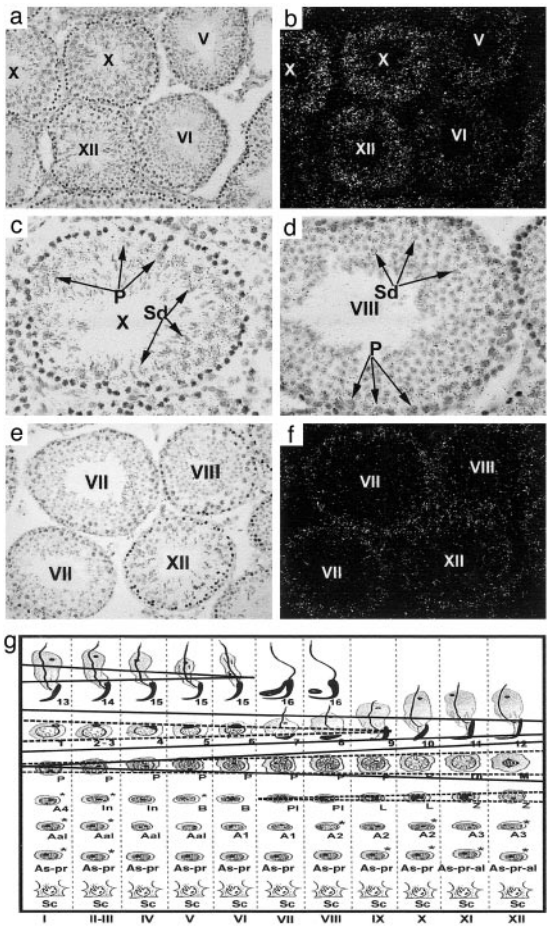

Fig. 3. Localization of mRNAs for α2 (*a–d*) and Lis1 and α1 (*e* and *f*) in adult mouse testes by *in situ* hybridization. Bright-field (*a* and *c–e*) and dark-field (*b* and *f*) images are shown. Higher levels of hybridization signals for α2 mRNA are observed over late pachytene spermatocytes (P) and lower levels over step 10 spermatids (Sd) at stage X of the epithelial cycle ($\times$100 in *a* and *b*; $\times$400 in *c*). At stage VIII ($\times$400 in *d*), similar levels of hybridization signals are over pachytene spermatocytes (P) and step-8 spermatids (Sd). α1 and Lis1 mRNAs display similar localization patterns, and, therefore, both are represented by the same images (*e* and *f*). The expression sites and levels of Lis1, α1, and α2 mRNAs are summarized in *g*. α1- and Lis1-expressing cells are framed with dashed lines, and α2-expressing cells are framed with solid lines. The width of the frame represents relative mRNA levels. The specific cell associations in the vertical columns represent specific stages (roman numerals) of the seminiferous epithelial cycle. Arabic numbers represent steps of spermatids. Sc, Sertoli cells; As, singled, type A spermatogonia; Apr, paired, type A spermatogonia; Aal, aligned, type A spermatogonia; A1–4, type A1–4 spermatogonia; In, intermediate spermatogonia; B, type B spermatogonia; Pl, preleptotene spermatocytes; L, leptotene spermatocytes; Z, zygotene spermatocytes; P, pachytene spermatocytes; Di, diplotene spermatocytes; M, meiotically dividing spermatocytes.

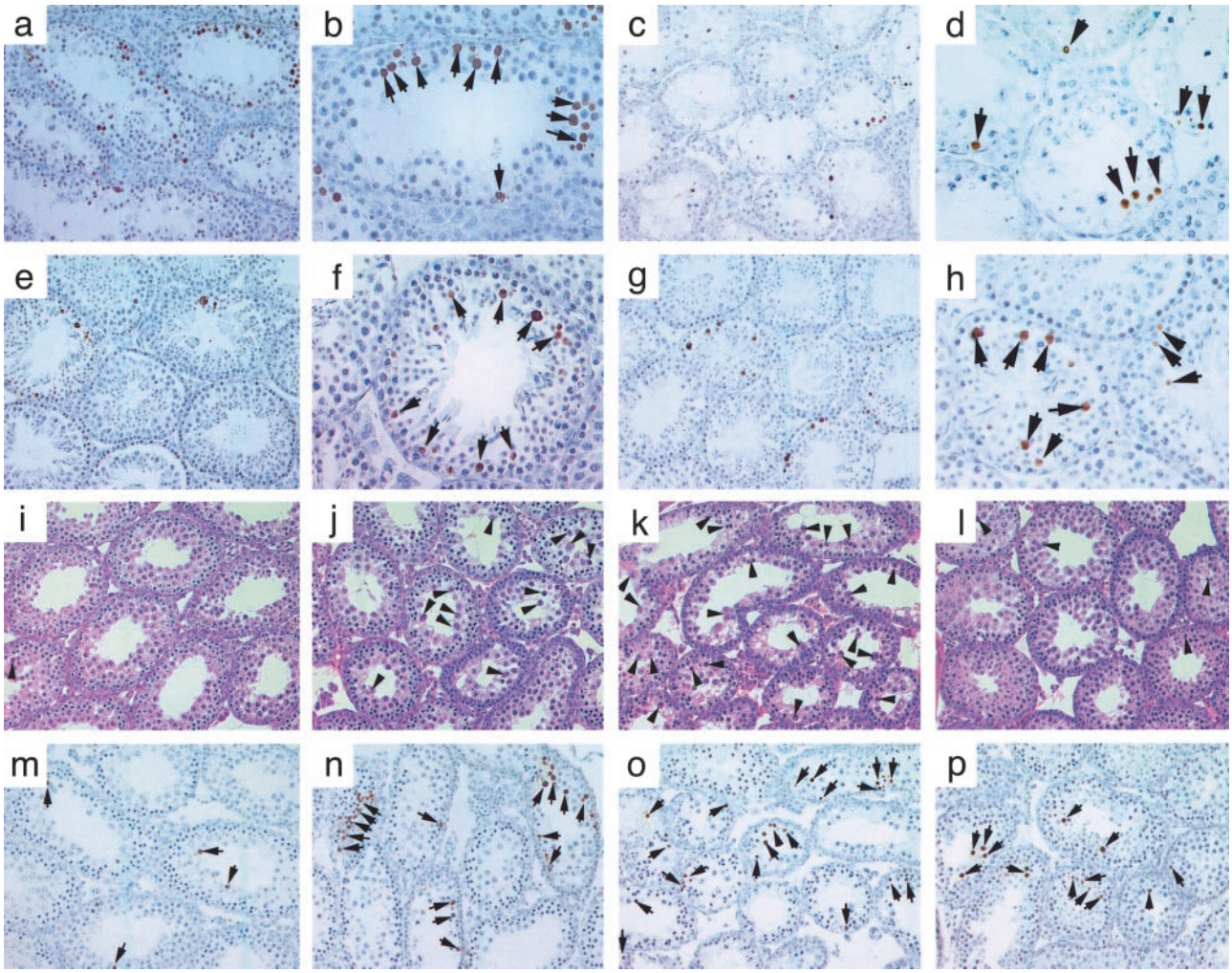

Fig. 4. Detection of germ cell apoptosis in wild-type and mutant testes. Lower-magnification (×200 in *a*, *c*, *e*, *g*, and *i–p*) and higher-magnification (×400 in *b*, *d*, *f*, and *h*) images are shown. Arrowheads (*i–l*) refer to morphologically degenerating germ cells, and arrows point to TUNEL-positive cells (brown). Morphology and TUNEL assay of adult (8-week-old) $\alpha2^{-/-}$ (*a* and *b*), double-mutant (*c* and *d*), triple-mutant (*e* and *f*), and $Lis1^{+/-}$ (*g* and *h*) testes are presented. Morphology and TUNEL assays of wild-type (*i* and *m*), $\alpha2^{-/-}$ (*j* and *n*), double-mutant (*k* and *o*), and triple-mutant (*l* and *p*) testes at P20 are shown.

produced $\alpha1^{-/-}\alpha2^{-/-}$ $Lis1^{+/-}$ mice (herein called triple-mutant mice). [Because of the embryonic lethality of $Lis1^{-/-}$ mice (10), triple-homozygous mice cannot be generated.] Interestingly, triple-mutant males were fertile although the testis weights of these mice (83.2 ± 7.3 mg, $n = 14$) was 20% less than wild-type mice (Fig. 2 *a* and *b*). Spermatogenesis in these triple-mutant males was well established and maintained although some degenerating germ cells and occasional multinucleated giant cells were observed in the seminiferous epithelium (Fig. 2*k*). Consistent with the normal fertility of these triple-mutant mice, the epididymides were full of spermatozoa (Fig. 2*l*). The testis morphology of the triple-mutant mice were similar to $Lis1^{+/-}$ mice, displaying a 35% reduction in weight (67.8 ± 10.2 mg, $n =$ 16), reduction in tubule diameters, and more degenerating germ cells (Fig. 2 *b*, *m*, and *n*). These results suggest that the levels of Lis1 influence the testis phenotypes in $\alpha2^{-/-}$ or $\alpha1^{-/-}\alpha2^{-/-}$ mice.

Disrupted Germ Cell Types Correlate with the Spatial Expression of Lis1, α1, and α2 in Mouse Testis. To understand further the phenotypes of the mutant mice, we analyzed the testicular expression of the PAFAH1B complex genes by *in situ* hybridization. α2 mRNA was the most abundant among the three genes in the testis, and it was detected in all pachytene spermatocytes, diplotene spermatocytes, meiotically dividing spermatocytes, and all spermatids (Fig. 3 *a–d* and *g*). Lis1 and α1 displayed similar expression patterns. Both mRNAs were expressed at lower levels in the testis and confined to all spermatocytes and spermatids up to step 9 (Fig. 3 *e–g*). The higher expression of α2 from late pachytene through meiotic division until the round spermatid stages is well correlated with the depletion of late pachytene spermatocytes through early spermatids in the seminiferous epithelium of the $\alpha2^{-/-}$ mice. This suggests that α2 plays a role in male germ cell meiosis during the late pachytene stage and meiotic divisions as well as early spermiogenesis. The more severe depletion of early spermatocytes including preleptotene, leptotene, zygotene spermatocytes in the double-mutant mice (Fig. 2 *i* and *j*) was well correlated with the earlier onset of α1 expression in the testis, implying that lack of α1 has a synergistic effect in the absence of α2.

Degeneration of Germ Cells in PAFAH1B Complex Mutant Mice Is Mediated Through Apoptosis. To determine the nature of the germ cell degeneration, we performed TUNEL analysis on these mutant testes (Fig. 4). Physiological apoptosis is present in spermatogonia, preleptotene, leptotene, zygotene, pachytene

(only at stages I and XII), and meiotically dividing spermatocytes (stage XII); TUNEL-positive germ cells normally are present at 0–7 per 100 Sertoli cells at each stage of the epithelial cycle (17). We conducted quantitative analyses by counting the number of Sertoli cells and TUNEL-positive germ cells in 100 tubule cross sections and converting the results into the number of TUNEL-positive germ cells per 100 Sertoli cells in the mutant and wild-type testes at 8 weeks of age. $\alpha2^{-/-}$ testes displayed a 30-fold increase in the number of TUNEL-positive germ cells that morphologically resembled pachytene spermatocytes (Fig. 4 *a* and *b*). Interestingly, some multinucleated giant cells were TUNEL-negative, suggesting that these unique structures degenerated via a mechanism different from conventional apoptosis (20). Examination of the $\alpha1^{-/-}\alpha2^{-/-}$ testes revealed a 10-fold increase in TUNEL-positive germ cells that appeared to be early spermatocytes including preleptotene, leptotene, and zygotene spermatocytes (Fig. 4 *c* and *d*), further suggesting redundant interactions of $\alpha1$ and $\alpha2$ in spermatogenesis. In triple-mutant testes, the number of TUNEL-positive germ cells, mainly pachytene spermatocytes, were 5-fold higher than in wild-type (Fig. 4 *e* and *f*), which is similar to $Lis1^{+/-}$ testes (Fig. 4 *g* and *h*).

Disruption of Spermatogenesis Occurs at the Initiation Phase in $\alpha2^{-/-}$ and $\alpha1^{-/-}\alpha2^{-/-}$ Mice. Spermatogenesis can be divided into two developmental phases: initiation (before 6 weeks of age) and maintenance (after 6 weeks of age). To determine the onset of disruption of spermatogenesis in these mutant mice, we analyzed the testes at postnatal day (P)12 and P20. At P12, preleptotene, leptotene, and zygotene spermatocytes are present in the seminiferous epithelium and occasionally early pachytene spermatocytes start to appear in some tubules. Histological examination demonstrated no difference in the testicular morphology among these mutant mice and wild-type mice (data not shown). At P20, germ cells have completed the first round of meiotic division and haploid germ cells appear in the seminiferous tubules in wild-type mice (Fig. 4*i*). A few apoptotic pachytene spermatocytes occasionally are present in the tubules (Fig. 4*m*). In the $\alpha2^{-/-}$ testis at P20 (Fig. 4 *j* and *n*), numerous pachytene spermatocytes and round spermatids are degenerating (Fig. 4*j*), as confirmed by TUNEL staining (Fig. 4*n*). In the double-mutant testis at P20, most of pachytene spermatocytes had been depleted, leaving fewer germ cells in the seminiferous epithelium (Fig. 4 *k* and *o*), as compared with wild-type (Fig. 4*i*) or $\alpha2^{-/-}$ testis (Fig. 4*j*) at P20. Early spermatocytes, including preleptotene, leptotene, and zygotene spermatocytes, also are degenerating (Fig. 4*k*), consistent with TUNEL-staining analysis (Fig. 4*o*). In the triple-mutant testis at P20, the morphology of the seminiferous tubules (Fig. 4*l*) is similar to wild-type testis (Fig. 4 *i* and *m*) except there are more TUNEL-positive spermatocytes (Fig. 4*p*). These findings demonstrate that spermatogenesis was disrupted at the initiation phase of spermatogenesis in $\alpha2^{-/-}$ and $\alpha1^{-/-}\alpha2^{-/-}$ mice. The disruption occurred earlier in $\alpha1^{-/-}\alpha2^{-/-}$ testes than in $\alpha2^{-/-}$ testes, suggesting further a synergistic role of $\alpha1$ in the $\alpha2^{-/-}$ background.

Expression of Testicular Marker Genes in the Mutant Mice. The most severely affected germ cell populations in the $\alpha2^{-/-}$ or the $\alpha1^{-/-}\alpha2^{-/-}$ testes appeared to be pachytene spermatocytes and round spermatids. Northern blot analysis confirmed the histological findings (Fig. 5*a*). Protamine 1 [*Prm1*, expressed in step 7–16 spermatids (22)], Testis-specific polyadenylate polymerase [*Tpap*, expressed in step 1–7 round spermatids (23)], and Zinc finger protein 393 [*Zfp393*, expressed in step 4–7 spermatids (14)] are much lower in the $\alpha2^{-/-}$ and double-mutant testes than in wild-type, triple-mutant, and $Lis1^{+/-}$ testes. *Gasz*, a germ cell-specific gene encoding a protein with four ankyrin repeats, a sterile-α motif, and a basic leucine zipper, is expressed in pachytene spermatocytes and step 1–2 spermatids in the mouse testis (16). *Gasz* mRNA levels are reduced dramatically in the $\alpha2^{-/-}$ testes, and the levels of *Gasz* mRNA are barely detectable in $\alpha1^{-/-}\alpha2^{-/-}$ testes, consistent with depletion of early pachytene spermatocytes (Fig. 5*a*). These results are consistent with the depletion of spermatocytes and spermatids in $\alpha2^{-/-}$ and $\alpha1^{-/-}\alpha2^{-/-}$ mice and their reappearance in triple mutant mice.

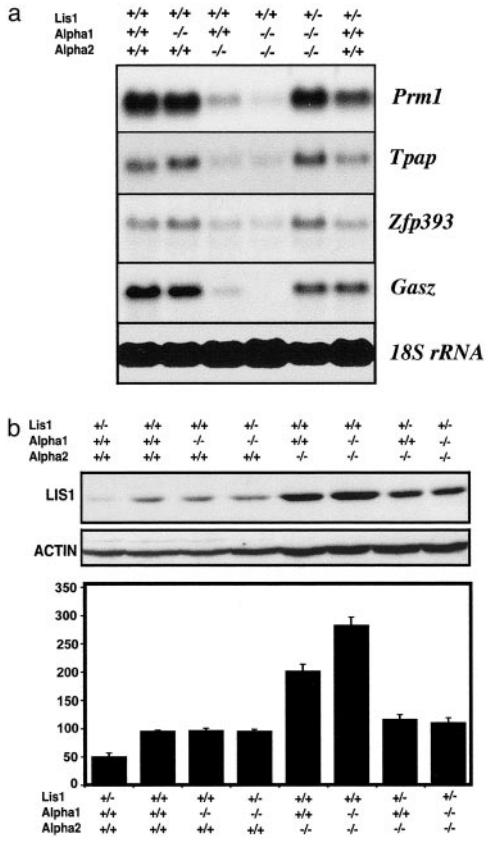

Fig. 5. Expression of testicular marker genes and Lis1 protein. (*a*) Northern blot analysis of *Prm1*, *Tpap*, *Zfp393*, *Gasz*, and 18S rRNA in wild-type and mutant testes. (*b*) Representative Western blot analysis of Lis1 and actin protein levels in wild-type and mutant testes at P12 (*Top* and *Middle*). (*Bottom*) Histogram showing the quantitative analysis of LIS1 protein levels of three independent experiments (means ± SEM, $n = 3$). ADU, arbitrary densitometric values standardized with actin loading controls.

Up-Regulation of LIS1 in $\alpha2^{-/-}$ and $\alpha2^{-/-}/\alpha1^{-/-}$ Testes and Rescue of the $\alpha2^{-/-}$ Defects by Lowering LIS1 Levels. Because the testicular phenotype caused by absence of $\alpha2$ was rescued by inactivating one allele of Lis1, we considered the possibility that $\alpha2$ disruption of spermatogenesis may result from overexpression of Lis1. It is impossible to quantify the Lis1 protein levels in the adult mutant testes because germ cells that express Lis1 (spermatocytes and round spermatids) are severely depleted in $\alpha2$ and $\alpha1/\alpha2$ double knockouts. The onset of germ cell depletion was around P15, when middle or late pachytene spermatocytes appear in the developing testes. Lis1 also is expressed in preleptotene, leptotene, zygotene, and early pachytene spermatocytes, and these germ cells are present and abundant in the mutant testes at P12. Therefore, we analyzed the expression levels of Lis1 in wild-type and mutant mice at P12 (Fig. 5*b*). The Lis1 protein levels in the $Lis1^{+/-}$ testis appeared to be reduced to approximately half the levels in wild-type testis, and no changes in Lis1 protein were observed in the $\alpha1^{-/-}$ testis. Testicular Lis1 protein levels at P12 were elevated markedly in the $\alpha2^{-/-}$ and double-mutant mice compared with wild-type mice (Fig. 5*b*).

LIS1 levels in the triple-mutant testes were slightly higher than those in the wild-type testes. These data suggest that the testicular phenotypes of the $\alpha 2^{-/-}$ or the double-mutant testis result from up-regulated Lis1 levels, and the testicular phenotypes of the $\alpha 2^{-/-}$ or the double-mutant mice are rescued by lowering Lis1 levels in the triple-mutant mice. It is also possible that increased levels of free LIS1, unbounded to PAFAH1B complex, is toxic to spermatogenic cells, especially to spermatocytes and spermatids. Interestingly, up-regulation of Lis1 mRNA levels also was observed in double-mutant testes but not in $\alpha 2^{-/-}$ testes (Fig. 1*e*), indicating complex control of expression of these genes.

The data presented here demonstrate that the PAFAH1B complex has an important role in spermatogenesis. The exact molecular event that this complex mediates in the testis is uncertain, but it is unlikely to involve solely the catalytic activity of PAFAH1B because the testicular phenotypes of nulls for both catalytic subunits are rescued by reduced levels of Lis1. It is more likely that PAFAH1B participates in spermatogenesis as a signaling complex by interacting with other intracellular proteins, as suggested previously (9). Interestingly, a recent study shows that overexpression of the receptor for very low density lipoprotein in mouse results in a testicular phenotype (24) similar to that reported here in $\alpha 2^{-/-}$ and $\alpha 1^{-/-}\alpha 2^{-/-}$ mice. We are conducting studies on the potential signaling pathways mediated through the PAFAH1B complex by standard genetic and biochemical strategies. These future studies would help us gain more insights into the molecular mechanisms by which the PAFAH1B complex and its interacting partners regulate spermatogenesis.

We thank L. Ma and R. S. McNeil for technical assistance and Dr. Ramiro Ramirez-Solis for support of these studies. This work was supported in part by National Institutes of Health Grants NS38389 (to G.D.C.), NS37146 (to G.D.C.), and HD33438 (to M.M.M.) and National Institutes of Health Specialized Cooperative Centers Program in Reproductive Research Grant HD07495. W.Y. is supported by a postdoctoral fellowship from the Ernst Schering Research Foundation. This work is an equal contribution of Baylor College of Medicine and the Max Planck Institute for Experimental Endocrinology (Hannover, Germany).

1. Amory, J. K. & Bremner, W. (2001) *Mol. Cell. Endocrinol.* **182,** 175–179.
2. Matzuk, M. M. & Lamb, D. J. (2002) *Nat. Med.* **8,** S41–S49.
3. Roudebush, W. E. (2001) *Asian J. Androl.* **3,** 81–85.
4. Cheminade, C., Gautier, V., Hichami, A., Allaume, P., Le Lannou, D. & Legrand, A. B. (2002) *Biol. Reprod.* **66,** 421–428.
5. Benoff, S. (1998) *Mol. Hum. Reprod.* **4,** 453–471.
6. Muguruma, K. & Johnston, J. M. (1997) *Biol. Reprod.* **56,** 529–536.
7. Palmer, J. S., Cromie, W. J., Plzak, L. F. & Leff, A. R. (1997) *J. Urol.* **158,** 1186–1190.
8. Arai, H., Koizumi, H., Aoki, J. & Inoue, K. (2002) *J. Biochem. (Tokyo)* **131,** 635–640.
9. Hattori, M., Adachi, H., Tsujimoto, M., Arai, H. & Inoue, K. (1994) *Nature* **370,** 216–218.
10. Hirotsune, S., Fleck, M. W., Gambello, M. J., Bix, G. J., Chen, A., Clark, G. D., Ledbetter, D. H., McBain, C. J. & Wynshaw-Boris, A. (1998) *Nat. Genet.* **19,** 333–339.
11. Abu-Issa, R. (2001) Ph.D. thesis (Baylor College of Medicine, Houston).
12. Matzuk, M. M., Finegold, M. J., Su, J. G., Hsueh, A. J. & Bradley, A. (1992) *Nature* **360,** 313–319.
13. Zambrowicz, B. P., Friedrich, G. A., Buxton, E. C., Lilleberg, S. L., Person, C. & Sands, A. T. (1998) *Nature* **392,** 608–611.
14. Yan, W., Burns, K., Ma, L. & Matzuk, M. (2002) *Mech. Dev.* **118,** 233–239.
15. Yan, W., Kero, J., Suominen, J. & Toppari, J. (2001) *Oncogene* **20,** 1343–1356.
16. Yan, W., Rajkovic, A., Viveiros, M. M., Burns, K. H., Eppig, J. J. & Matzuk, M. M. (2002) *Mol. Endocrinol.* **16,** 1168–1184.
17. Yan, W., Suominen, J., Samson, M., Jegou, B. & Toppari, J. (2000) *Mol. Cell. Endocrinol.* **165,** 115–129.
18. Chapin, R. E., Morgan, K. T. & Bus, J. S. (1983) *Exp. Mol. Pathol.* **38,** 149–169.
19. Singh, S. K. & Abe, K. (1987) *Arch. Histol. Jpn.* **50,** 579–585.
20. Print, C. G. & Loveland, K. L. (2000) *BioEssays* **22,** 423–430.
21. Totsuka, Y., Kawamori, T., Hisada, S., Mitsumori, K., Ishihara, J., Sugimura, T. & Wakabayashi, K. (2001) *Toxicol. Appl. Pharmacol.* **175,** 169–175.
22. Kleene, K. C., Distel, R. J. & Hecht, N. B. (1984) *Dev. Biol.* **105,** 71–79.
23. Kashiwabara, S., Zhuang, T., Yamagata, K., Noguchi, J., Fukamizu, A. & Baba, T. (2000) *Dev. Biol.* **228,** 106–115.
24. Tacken, P. J., van der Zee, A., Beumer, T. L., Florijn, R. J., Gijpels, M. J., Havekes, L. M., Frants, R. R., van Dijk, K. W. & Hofker, M. H. (2001) *Transgenic Res.* **10,** 211–221.